Cancer Therapy: Preclinical
See commentary by Crystal and Shaw, p. 4479

Clinical Cancer Research

Differential Protein Stability and ALK Inhibitor Sensitivity of EML4-ALK Fusion Variants

Johannes M. Heuckmann[1,4], Hyatt Balke-Want[1,4], Florian Malchers[1,4], Martin Peifer[1,4], Martin L. Sos[1,2,4], Mirjam Koker[1,4], Lydia Meder[3], Christine M. Lovly[5], Lukas C. Heukamp[3], William Pao[5], Ralf Küppers[6], and Roman K. Thomas[1,4]

Abstract

Purpose: *ALK* rearrangement–positive lung cancers can be effectively treated with ALK inhibitors. However, the magnitude and duration of response is heterogeneous. In addition, acquired resistance limits the efficacy of ALK inhibitors, with most upfront resistance mechanisms being unknown.

Experimental Design: By making use of the Ba/F3 cell line model, we analyzed the cytotoxic efficacy of ALK kinase inhibitors as a function of different *EML4-ALK* fusion variants *v1*, *v2*, *v3a*, and *v3b* as well as of three artificially designed *EML4-ALK* deletion constructs and the *ALK* fusion genes *KIF5b-ALK* and *NPM1-ALK*. In addition, the intracellular localization, the sensitivity to HSP90 inhibition and the protein stability of *ALK* fusion proteins were studied.

Results: Different *ALK* fusion genes and *EML4-ALK* variants exhibited differential sensitivity to the structurally diverse ALK kinase inhibitors crizotinib and TAE684. In addition, differential sensitivity correlated with differences in protein stability in *EML4-ALK*–expressing cells. Furthermore, the sensitivity to HSP90 inhibition also varied depending on the ALK fusion partner but differed from ALK inhibitor sensitivity patterns. Finally, combining inhibitors of ALK and HSP90 resulted in synergistic cytotoxicity.

Conclusions: Our results might explain some of the heterogeneous responses of *ALK*-positive tumors to ALK kinase inhibition observed in the clinic. Thus, targeted therapy of *ALK*-positive lung cancer should take into account the precise *ALK* genotype. Furthermore, combining ALK and HSP90 inhibitors might enhance tumor shrinkage in *EML4-ALK*–driven tumors. *Clin Cancer Res; 18(17); 4682–90. ©2012 AACR.*

Introduction

ALK gene fusions occur in 2% to 7% of lung adenocarcinomas (1, 2). These fusions are oncogenic *in vitro* and *in vivo* and cause oncogene dependency by constitutive kinase activation of the ALK tyrosine kinase (1, 3). All preclinical models show that ALK fusion–positive tumor cells are exquisitely sensitive to ALK kinase inhibition (1, 4, 5). Furthermore, a phase I/II study in advanced, *ALK*-positive, non–small cell lung cancer showed dramatic radiographic responses using the ALK tyrosine kinase inhibitor crizotinib (PF02341066; ref. 2). However, more recent studies suggest more heterogeneous responses to this inhibitor (6).

ALK was first discovered in a gene fusion with nucleophosmin (*NPM1*) in anaplastic large-cell lymphoma, giving this gene its name (anaplastic lymphoma kinase; ref. 7). The predominant 5′-partner in *ALK* fusion–positive lung cancer involves echinoderm microtubule–associated protein like-4 (*EML4*), with few reported cases harboring an *ALK* fusion with kinesin family member 5B (*KIF5b*; ref. 8). Several different *EML4-ALK* variants have been described, with *variant 1* (*v1*, 33%), *variant1* (*v2*, 10%), and *variants 3 a/b* (*v3a/v3b*, 29%) being the most frequent fusions (9, 10). All variants contain exons 20–29 of *ALK* (which encode the entire ALK tyrosine kinase domain) fused to a varying proportion of *EML4* (3). EMLs are believed to represent a class of microtubule destabilizers, even though their exact function remains unknown (11). The proportion of *EML4* fused to the kinase domain of *ALK* varies depending on the respective fusion variant, whereas the coiled–coiled domain of *EML4* seems to be essential for homodimerization and kinase activation (1). Importantly, all *EML4-ALK* fusion variants studied so far are oncogenic and all induce ALK dependency (3, 5).

Despite the initial success of ALK inhibitors in *ALK* fusion–positive lung cancer, it is presently unclear whether

Authors' Affiliations: [1]Department of Translational Genomics, [2]Department I of Internal Medicine and Center of Integrated Oncology Köln–Bonn, [3]Institute of Pathology, University of Cologne; [4]Max Planck Institute for Neurological Research; [5]Department of Hematology and Oncology, Vanderbilt University School of Medicine Nashville, Tennessee; and [6]Institute of Cell Biology (Cancer Research), University of Duisburg-Essen, Medical School, Essen, Germany

Note: Supplementary data for this article are available at Clinical Cancer Research Online (http://clincancerres.aacrjournals.org/).

Current address for Martin L. Sos: Howard Hughes Medical Institute, Department of Cellular and Molecular Pharmacology, University of California, San Francisco, California 94158, USA

Corresponding Author: Roman K. Thomas, Department of Translational Genomics, University of Cologne, c/o MPI for Neurological Research, Gleueler Str. 50, 50931 Cologne, Germany. Phone: 49-221-478-98771; Fax: 49-221-478-98771; E-mail: roman.thomas@uni-koeln.de

doi: 10.1158/1078-0432.CCR-11-3260

Translational Relevance

Lung cancers with *ALK* rearrangements are sensitive to ALK inhibitors but responses are heterogeneous. Here, we show that *EML4-ALK* variants show differential sensitivity to ALK and HSP90 inhibitors. These phenotypes were independent of inhibitor scaffold and binding mode. Furthermore, a combination of ALK and HSP90 inhibitors led to synergistic cytotoxicity in *ALK* fusion gene-expressing cells. Thus, the application of ALK and HSP90 inhibitors might have to be adapted to the precise variant of *ALK* fusion to enhance tumor control and optimize patient benefit in lung cancer.

the different variants impact the therapeutic efficacy of ALK inhibition (10). In light of the differential sensitivity of various EGF receptor (EGFR) mutants to EGFR inhibition (12–14), we sought to determine the responsiveness of various *EML4-ALK* fusion variants to structurally diverse ALK inhibitors. Furthermore, we aimed at providing mechanistic insight into any potential differences in inhibitor sensitivity.

Materials and Methods

cDNA and cell lines

pMA-3FLAG-*EML4-ALK v1/v2/v3b*, *BCR-ABL*, *NPM1-ALK*, and *KIF5b-ALK* cDNAs were cloned into the retroviral pBabe puro backbone. Site-directed mutagenesis was carried out as described previously to generate pBabe puro *EML4-ALK v3a* from pBabe puro *EML4-ALK v3b*, pBabe puro *EML4-ALK del223* from pBabe puro *EML4-ALK v3a*, pBabe puro *EML4-ALK del346*, and *702* from pBabe puro *EML4-ALK v2* (15). Ba/F3 and NIH3T3 cell lines were established as described previously (15, 16).

Compounds

Compounds were purchased from commercial suppliers or extracted from tablets and diluted in dimethyl sulfoxide (DMSO). Bortezomib was a kind gift from Nina Reinart, Fingerle-Rowson Lab, Klinik I für Innere Medizin, Uniklinik Köln, Germany.

Immunoblotting

Immunoblotting was done using standard procedures (17). The following antibodies were used: pALK (Tyr1604), pAKT (Ser473), AKT, pERK, and ERK from Cell Signaling, actin from MP Biomedical, and total ALK from Bethyl Laboratories. Signal intensities were measured using ImageJ (1.42q).

Immunohistochemistry

NIH3T3 cells expressing the respective transgene were seeded on 22-mm diameter glass slides. After 24 hours of incubation, slides were fixed in 4%PFA for 15 minutes before incubation with PBS + 0.2% TritonX for 5 minutes. Primary antibody incubation was carried out in a humified chamber for 1 hour at room temperature. Fluorescein isothiocyanate (FITC)-labeled secondary antibody plus 4′, 6-diamidino-2-phenylindole (DAPI) staining was carried out for 45 minutes in a dark humified chamber before covering slides on coverslips with SlowFade Gold (Invitrogen). Pictures were taken on an Aristoplan machine (Leica/Leitz Microsystems).

Viability assays

Ba/F3 viability assays were carried out as described previously (18) measuring cellular ATP content (Cell- Titer-Glo; Promega) after 72 hours or 96 hours of treatment.

Domain search

Protein domains were searched using **S**imple**M**odular-**A**rchitecture**R**esearch**T**ool (http://smart.embl-heidelberg.de/)

Results

To test whether different *EML4-ALK* fusion variants exhibit differential sensitivity to ALK inhibition in a defined cellular background, we made use of the Ba/F3 cell line model (15). All 4 different *EML4-ALK* variants studied (*v1*, *v2*, *v3a*, and *v3b*) rendered Ba/F3 cells independent of addition of exogenous interleukin 3 (IL3) and showed similar proliferation rates (Supplementary Fig. S1). *EML4-ALK* variants *v1* and *v3b* showed no significant differences in the half-maximal growth inhibitory concentration ("GI_{50} values") when treated with the aminopyridine ALK inhibitor crizotinib (PF02341066; GI_{50} values 470 nmol/L, Fig. 1A). Surprisingly, Ba/F3 cells expressing *v2* and *v3a* showed considerable differences in sensitivity to ALK kinase inhibition (GI_{50} 150 and 1,000 nmol/L, respectively; Fig. 1A). The same pattern of sensitivity was observed in cells treated with the structurally different diaminopyrimidine ALK kinase inhibitor TAE-684 with GI_{50} values ranging from 0.3 nmol/L for *variant 2* to 24 nmol/L for *variant 3a* (Fig. 1A), indicating that the differences in sensitivity were independent of the binding mode of the inhibitor (19). To determine whether the accessibility or the binding affinity of the inhibitors to the ATP-binding pocket differs in these variants, we carried out immunoblotting to monitor ALK phosphorylation of *variant 2* and *variant 3a* after 1 hour of ALK kinase inhibitor treatment. As has been shown for another ALK kinase inhibitor, both variants, expressed in Ba/F3 cells, showed the same pattern of ALK phosphorylation with kinase inhibition at crizotinib concentrations as low as 300 nmol/L (Fig. 1B; ref. 20). To verify these results in a different cell type, *variants 2* and *3a* were expressed in NIH3T3 cells. After 1 hour of treatment, *variant 2* and *variant 3a* again showed no differences in ALK phosphorylation after crizotinib treatment (Fig. 1C, Supplementary Fig. S2A). As has already been shown for *EML4-ALK*–expressing NIH3T3 cells, in both variants ALK kinase inhibition led to a dose-dependent dephosphorylation of ERK, whereas levels of phosphorylated AKT remained almost unchanged after treatment (Supplementary Fig.

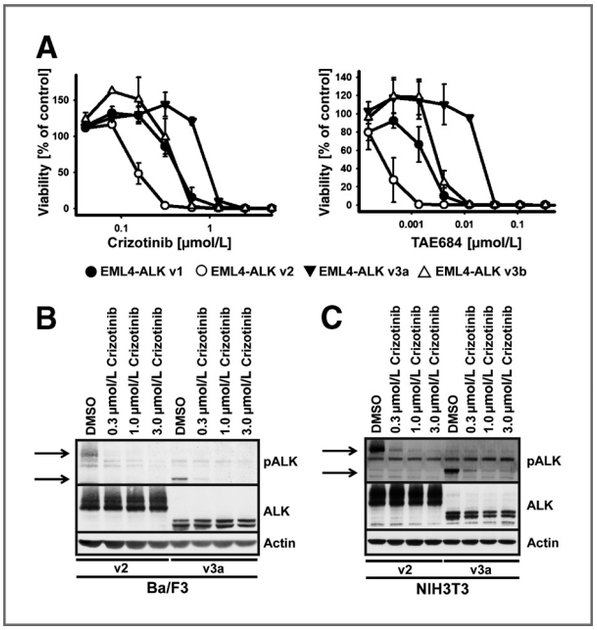

Figure 1. ALK inhibitor sensitivity of *EML4-ALK* variants. A, Ba/F3 cells expressing the indicated *EML4-ALK* variants were treated with increasing concentrations of crizotinib (left) or TAE684 (right). Viability was determined after 96 hours by measurements of cellular ATP content and expressed as a function of compound dose relative to the viability of the DMSO-treated controls. Each data point represents the mean of 3 independent triplicate measurements, error bars indicate SEM. B, Ba/F3 cells expressing the indicated *EML4-ALK* cDNAs were treated with crizotinib for 1 hour. Whole-cell lysates were prepared and analyzed for pALK, ALK, and actin protein levels by immunoblotting. C, whole-cell lysates of NIH3T3 cells stably expressing *EML4-ALK v2* and *v3a* were treated with different concentrations of crizotinib for 1 hour. Levels of ALK phosphorylation were monitored by immunoblotting. Actin was used as loading control.

S2A; ref. 21). In line with these findings, a comparison of *variant 1* and *variant 3a* yielded the same results (Supplementary Fig. S2B). These results suggested that inhibitor binding to the kinase domain is similar in all EML4-ALK variants tested.

Due to the fact that all *EML4-ALK* variants harbor the complete kinase domain of *ALK* (exon 20 to exon 29), we hypothesized that the observed differences in inhibitor sensitivity might be mediated by the proportion of *EML4* that is fused to *ALK* (Supplementary Fig. S3). In addition to the coiled–coiled domain, which is essential for the oncogenic capacity of EML4-ALK (1), EML4 contains one HELP domain as well as 9 WD40 domains. The HELP domain of EML4 has been reported to mediate tubulin binding (11), whereas WD40 domains are known to mediate a variety of protein–protein interactions that are difficult to predict (22). To determine whether any of these domains mediate differences in intracellular localization and thereby could explain the observed phenotypes, we stained for ALK in *EML4-ALK*–expressing NIH3T3 cells by immunohistochemistry. EML4-ALK variants 1 and 2 were abundant in the cytoplasm, with only minimal staining in the nucleus (Fig. 2A). However, v3a was equally distributed throughout the cytoplasm and the nucleus, suggesting that the HELP domain (present in v1 and v2, but not in v3a) retains the fusion protein in the cytoplasm (Fig. 2A, Supplementary Fig. S3; ref. 11). Because EML4-ALK variant 1 and variant 2 showed no differences in intracellular distribution but showed considerable differences in kinase inhibitor sensitivity, the impact of the intracellular distribution is likely of minor relevance to ALK kinase inhibitor sensitivity.

In addition to short-term kinase inhibitor treatment, we carried out immunoblotting of ALK in whole-cell lysates of *EML4-ALK*–expressing NIH3T3 cells after 24 hours of treatment to analyze the effects of longer kinase inhibition. Strikingly, total ALK levels were considerably decreased in variant 2 at 1 and 3 μmol/L of crizotinib (Fig. 2B). By contrast, the total amount of variant 3a was not reduced at concentrations of 1 μmol/L of crizotinib, with reduced total protein levels appearing only at 3 μmol/L of treatment (Fig. 2B). This dose-dependent effect of total ALK degradation was also present in Ba/F3 cells and was again much more pronounced in variant 2 compared with variant 3a (Fig. 2C). High-dose treatment with TAE684 for 24 hours recapitulated this observation (Supplementary Fig. S4). To analyze overall ALK protein stability in

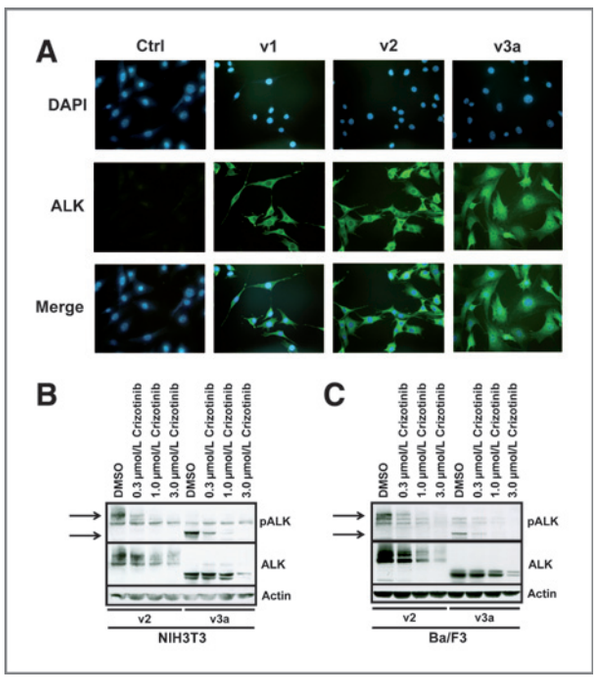

Figure 2. Intracellular distribution of *EML4-ALK* variants and crizotinib-induced ALK protein degradation. A, NIH3T3 cells expressing the indicated *EML4-ALK* variants were fixed on glass slides and stained for total ALK (FITC, green) and nuclei (DAPI, blue). Pictures were taken on an Aristoplan machine (Leica/Leitz Microsystems) at 400-fold magnification. B, NIH3T3 cells expressing the indicated *EML4-ALK* cDNAs were treated with increasing concentrations of crizotinib. After 24 hours of treatment, lysates were prepared and analyzed for pALK, ALK, and actin protein levels by immunoblotting. C, Ba/F3 cells stably expressing *EML4-ALK v2* and *v3a* were treated with different concentrations of crizotinib for 24 hours. Levels of ALK phosphorylation and of total ALK were determined by immunoblotting. Actin was used as loading control.

more detail, we treated *EML4-ALK*–expressing Ba/F3 and NIH3T3 cells with 50 or 100 μg/mL of cycloheximide for 24 hours. Immunoblotting of ALK revealed remarkable differences in the amount of total ALK protein when comparing cycloheximide and untreated cell lysates. *EML4-ALK variant 2*–expressing cells showed the most pronounced differences in the amount of total ALK protein between untreated and treated cells, whereas cells expressing *EML4-ALK variants 3a* showed the least differences. These data showed that EML4-ALK variant 2 has a shorter half-life compared with the other variants (Fig. 3A, Supplementary Fig. S5). Thus, binding of crizotinib to the kinase domain of EML4-ALK variant 2 accelerates protein degradation at much lower concentrations compared with variant 3a. Furthermore, our data suggested that the proportion of *EML4* that is fused to *ALK* defines the general stability of the resulting fusion protein.

Previous studies have shown that total EML4-ALK levels decrease after treatment with HSP90 inhibitors (23–25). In light of our cycloheximide studies, we asked whether the different *EML4-ALK* variants display differential sensitivity to HSP90 inhibition as well. We treated Ba/F3 cells expressing *EML4-ALK variants 2* and *3a* with increasing concentrations of the ansamycin antibiotic derivative HSP90 inhibitor, 17-DMAG. As predicted, *variant 2* was more sensitive to HSP90 inhibition compared with *variant 3a*, which was almost as resistant as the IL3-supplemented control (Fig. 3B). Surprisingly, Ba/F3 cells expressing *EML4-ALK variant 1* were as sensitive to 17-DMAG as *EML4-ALK v2*–expressing cells (Fig. 3C). Thus, the intrinsic stability of the fusion variants impacts their dependency on chaperonage by HSP90 but also show that other factors (e.g., intracellular distribution, Fig. 2A) may also influence HSP90 inhibitor sensitivity. Unfortunately, the high intrinsic sensitivity of all Ba/F3 cell lines to HSP90 inhibition (evidenced by the high sensitivity of IL3-supplemented Ba/F3 cells) limits the ability to document minor differences in sensitivity (i.e., *v1* vs *v2*). Experiments with a synthetic HSP90 inhibitor, AUY922, yielded similar results; however, the high sensitivity of IL3-supplemented controls made these experiments difficult to interpret (Supplementary Fig. S6).

To test, whether the observed EML4-ALK degradation depends on proteasome activity, we treated *EML4-*

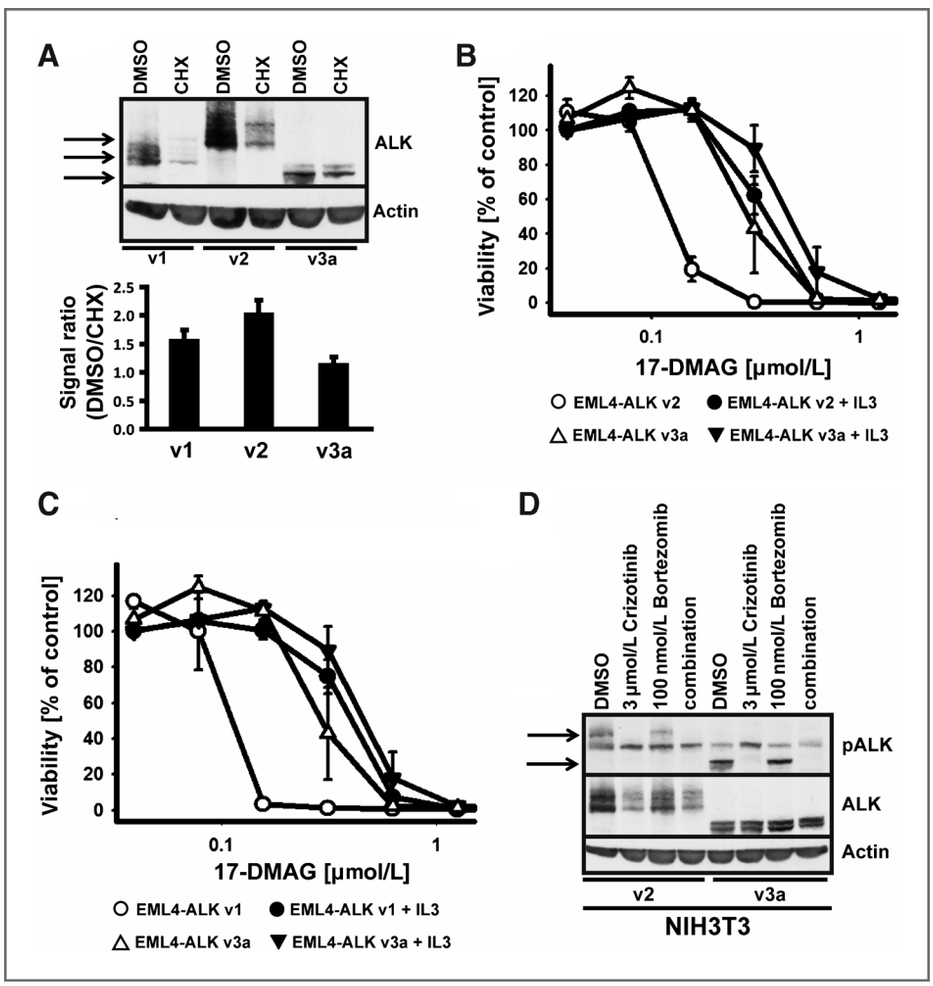

Figure 3. Protein stability of *EML4-ALK* variants. A, Ba/F3 cells expressing the indicated *EML4-ALK* variants were treated with DMSO or 50 μg/mL cycloheximide for 24 hours. Whole-cell lysates were prepared and stained for total ALK levels by immunoblotting. Signal intensity of staining was analyzed using ImageJ software. Signal ratios of DMSO/CHX are shown for 3 independent experiments, error bars indicate SEM. B and C, Ba/F3 cells expressing the indicated *EML4-ALK* variants were treated with increasing concentrations of 17-DMAG. Viability was determined after 72 hours by measurements of cellular ATP content and expressed as a function of compound dose relative to the viability of the DMSO-treated controls. Each data point represents the mean of 3 independent triplicate measurements; error bars indicate SEM. D, NIH3T3 cells expressing the indicated *EML4-ALK* cDNAs were treated with 3 μmol/L crizotinib, 100 nmol/L bortezomib, or both compounds combined. After 24 hours of treatment, lysates were prepared and analyzed for pALK, ALK, and actin protein levels by immunoblotting. CHX, cycloheximide.

ALK–expressing Ba/F3 cells with the proteasome inhibitor, bortezomib. Here, *v2* and *v3a* showed the same sensitivity. However, this effect could not be rescued by addition of IL3 and was therefore likely to be mediated by general cellular toxicity of bortezomib in these cells (Supplementary Fig. S7). To further analyze whether proteasome inhibition could rescue ALK inhibitor–induced EML4-ALK degradation, we treated EML4-ALK–expressing NIH3T3 cells with 3 μmol/L crizotinib, 100 nmol/L bortezomib, or both compounds combined for 24 hours. However, proteasome inhibition did not reduce crizotinib-induced protein degradation, implying that the degradation process is proteasome independent (Fig. 3D).

Because the longest variant (variant 2) was the least stable (Fig. 3A) and showed the highest degree of sensitivity to ALK inhibition (Fig. 1A), we hypothesized that variations at the N-terminal portion of *EML4-ALK* have the strongest impact on protein stability and thus, kinase inhibitor sensitivity. To confirm this hypothesis, we generated 3 artificial *EML4-ALK* deletion variants varying in the N-terminal part and by the number of WD40 domains (Fig. 4A). We used *variant 2* as a template to remove amino acids 299–346 (*del346*, lacking the first WD40 domain adjacent to the HELP domain) or 299–702 (*del702*, lacking the first 5 WD40 domains), and *variant 3a* was used to remove amino acids 61–223 (*del223*) to generate an *EML4-ALK* variant similar to *variant 5*. All

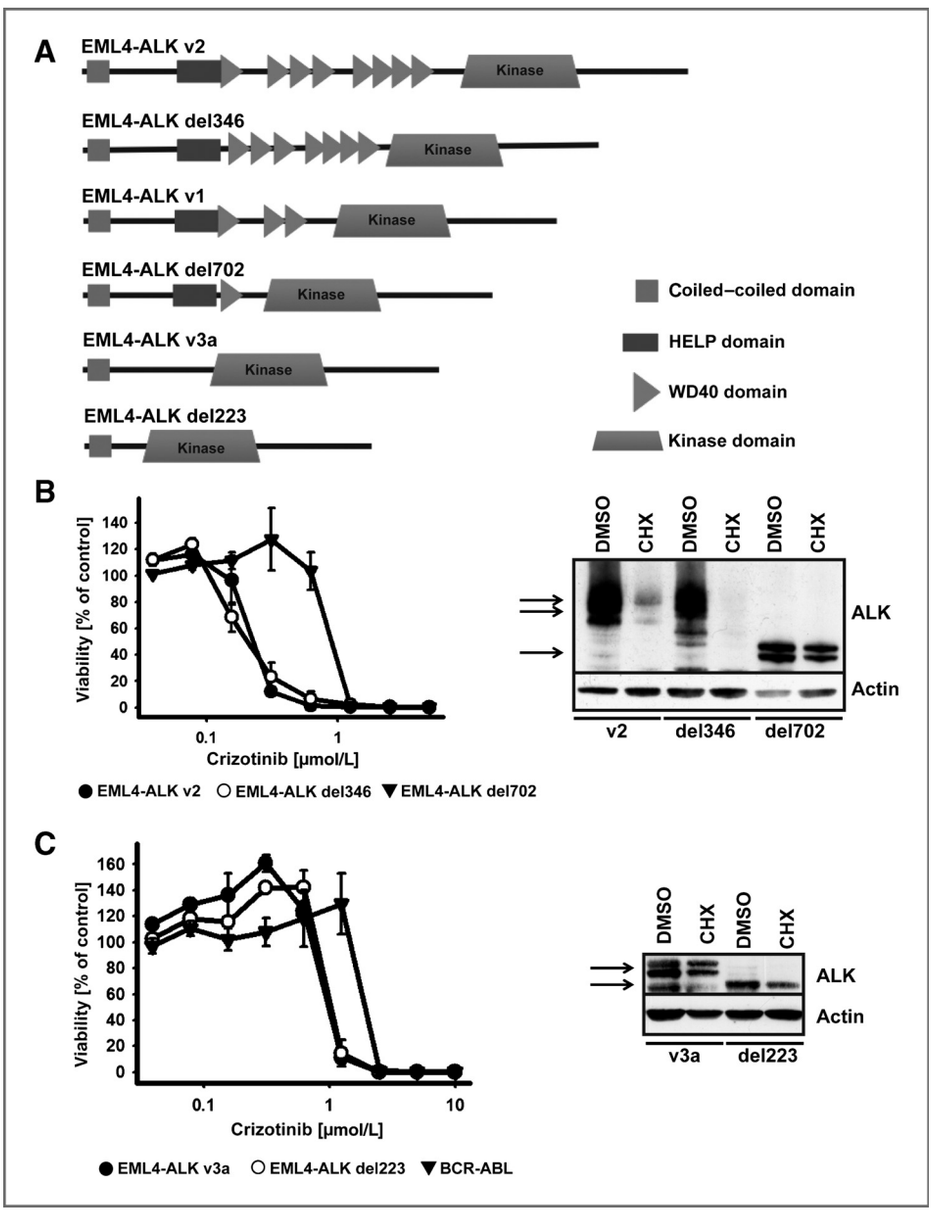

Figure 4. ALK inhibitor sensitivity and protein stability of *EML4-ALK* deletion variants. A, schematic representation of *EML4-ALK* variants and the deletion constructs *EML4-ALK del346*, *del702*, and *del223*. B and C, Ba/F3 cells expressing the indicated *EML4-ALK* deletion variants were treated with increasing concentrations of crizotinib. Viability was determined after 72 hours by measurements of cellular ATP content and expressed as a function of compound dose relative to the viability of the DMSO-treated controls. Each data point represents the mean of 3 independent triplicate measurements, error bars indicate SEM (left). Ba/F3 cells expressing the indicated *EML4-ALK* deletion variants were treated with DMSO or 50 μg/mL cycloheximide for 24 hours. Whole-cell lysates were prepared and stained for total ALK levels by immunoblotting (right). CHX, cycloheximide.

deletion constructs transformed Ba/F3 cells but showed a distinct sensitivity pattern after treatment. *EML4-ALK del346*–expressing Ba/F3 cells were as sensitive as *variant 2*–expressing cells after ALK kinase inhibition (Fig. 4B). By contrast, *del702*–expressing cells were much less sensitive to kinase inhibition compared with cells expressing *variant 2* (Fig. 4B). Furthermore, EML4-ALK del346 was the least stable protein following cycloheximide-mediated inhibition of translation, whereas EML4-ALK del702 showed almost no degradation, similar to variant 3a (Fig. 4B). Ba/F3 cells expressing *EML4-ALK del223* showed no difference in crizotinib sensitivity or protein stability compared with *variant 3a* (Fig. 4C). As expected, *EML4-ALK del223* and *v3a* showed a higher sensitivity to ALK inhibition compared with *BCR-ABL*–expressing cells, indicating that even though these variants induced the highest degree of resistance, they still exhibit sensitivity toward ALK inhibitors (Fig. 4C).

To test, whether other fusion partners and absolute protein size of the resulting fusion dictate sensitivity to ALK inhibition, we tested the sensitivity of *KIF5b-ALK* and *NPM1-ALK*–expressing Ba/F3 cells to crizotinib (Fig. 5A). Ba/F3 cells expressing *KIF5b-ALK* were highly sensitive to ALK inhibition, whereas *NPM1-ALK*–expressing cells showed an intermediate sensitivity compared with *variant 2* and *variant 3a* of *EML4-ALK* (Fig. 5B). Thus, the actual fusion partner and the domain composition—rather than the size of the fusion protein—dictate sensitivity to ALK inhibition. Cycloheximide treatment revealed a similar protein stability of the KIF5b-ALK and NPM1-ALK fusion proteins, despite the differences in ALK inhibitor sensitivity. Compared with EML4-ALK v2, both ALK fusion proteins were much more stable, indicating only a correlation between ALK inhibitor sensitivity and protein stability in *EML4-ALK*–expressing cells (Fig. 5C).

Because sensitivity to ALK kinase inhibition did not correlate with sensitivity to HSP90 inhibition, suggesting different mechanisms (Fig. 1A, Fig. 3B and C), we asked whether a combination of ALK and HSP90 inhibitors might induce additive cytotoxic effects. To this end, we treated Ba/F3 cells expressing *EML4-ALK v1*, *EML4-ALK v2*, and *v3a* as well as *KIF5b-ALK* and *BCR-ABL* with increasing concentrations of crizotinib, 17-DMAG, or both compounds combined, each at the same concentrations. Interestingly, in all *ALK* fusion gene–expressing cells, the combination of both compounds induced synergistic cytotoxicity (Fig. 6A and B, Supplementary Table S1; ref. 26). However, we note that the degree of synergy varied depending on the respective *ALK* fusion variant, with only minimal synergistic cytotoxicity observed in cells expressing *EML4-ALK v1*. As expected, in *BCR-ABL*–expressing cells, only treatment with 17-DMAG–induced cytotoxicity, which could not be enhanced further by combination treatment (Fig. 6A and B).

Collectively, our data showed that variations at the N-terminal part of *ALK* fusion genes strongly impact protein stability, HSP90 and kinase inhibitor sensitivity.

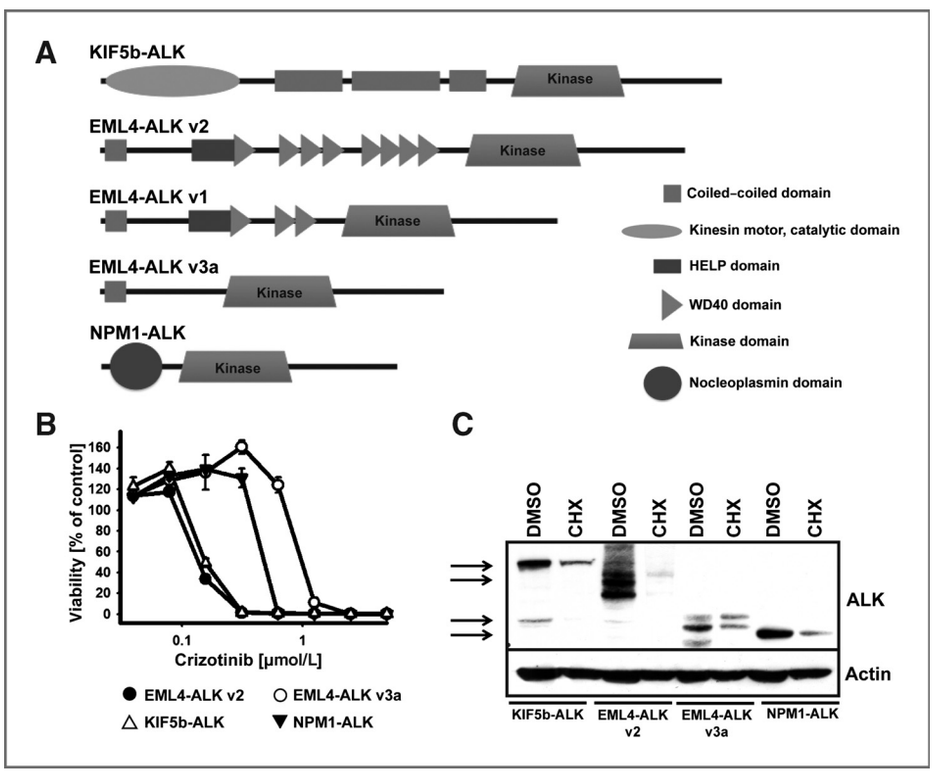

Figure 5. ALK inhibitor sensitivity and protein stability of KIF5b-ALK and NPM1-ALK. A, schematic representation of *EML4-ALK* variants, *KIF5b-ALK*, and *NPM1-ALK*. B, Ba/F3 cells expressing the indicated *ALK* fusions were treated with increasing concentrations of crizotinib. Viability was determined after 72 hours by measurements of cellular ATP content and expressed as a function of compound dose relative to the viability of the DMSO-treated controls. Each data point shows the mean of 2 independent triplicate measurements, error bars indicate SEM. C, Ba/F3 cells expressing the indicated *ALK* translocation were treated with DMSO or 50 μg/mL cycloheximide for 24 hours. Whole-cell lysates were prepared and stained for total ALK levels by immunoblotting. CHX, cycloheximide.

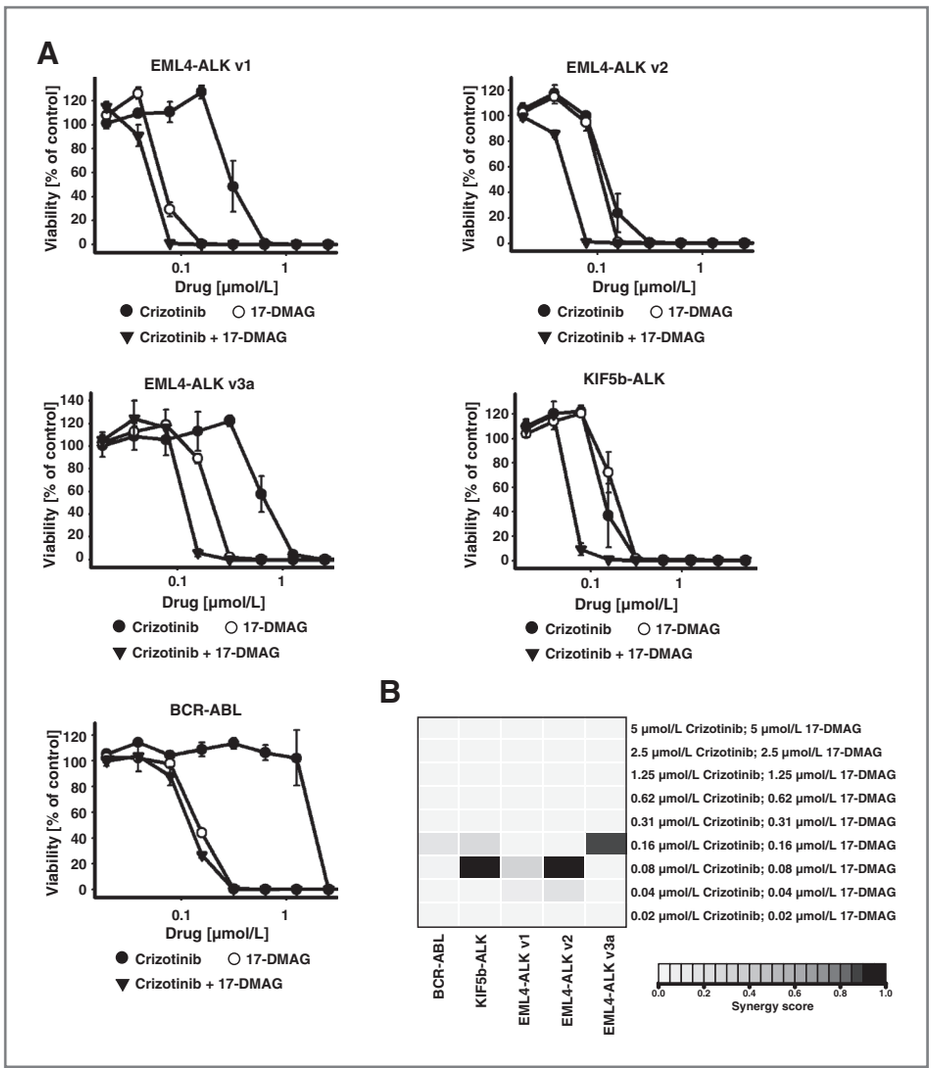

Figure 6. Synergistic cytotoxicity of ALK and HSP90 inhibitors in ALK fusion gene–expressing cells. A, Ba/F3 cells expressing the indicated cDNAs were treated with increasing concentrations of crizotinib, 17-DMAG, or a combination of both compounds at equal concentrations. Viability was determined after 96 hours by measurements of cellular ATP content and expressed as a function of compound dose relative to the viability of the DMSO-treated controls. Each data point shows the mean of 2 independent triplicate measurements, error bars indicate SEM. B, synergy strength scores were computed as described previously (25) and depicted as a heatmap.

Discussion

Here, we report differences in the sensitivity of different *EML4-ALK* variants to 2 structurally diverse ALK inhibitors crizotinib (aminopyridine) and TAE684 (diaminopyrimidine). These differences do not seem to be mediated by differential compound activity on the kinase. By contrast, we find that various parts of *EML4* that are fused to *ALK* in the different variants influence overall fusion protein stability, inhibitor-induced protein degradation, and drug sensitivity. These observations are also supported by analyses of artificial variants of various lengths as well as of the fusion genes *KIF5b-ALK* and *NPM1-ALK* that recapitulate our findings. However, a correlation between protein stability and ALK inhibitor sensitivity could only be shown for EML4-ALK.

We speculate that protein-folding properties of the somatically acquired (i.e., not evolutionary developed) fusions might lead to an open conformation, leaving several hydrophobic residues exposed. These exposed residues vary depending on the respective fusion variant and are likely to recruit HSP90 and other chaperones, which are essential for a stabilization of these proteins. This stabilization can effectively be disturbed by ALK or HSP90 inhibitors, initiating a proteasome-independent degradation of the fusion proteins. As a consequence, combined treatment of an ALK and HSP90 inhibitor induced synergistic cytotoxicity in all *ALK* fusion gene–expressing cells. The more similar the single drug GI_{50} values were, the higher the synergistic effect in the combination treatment with equal drug concentrations.

It remains to be seen whether our *in vitro* observations translate into the clinic. The previously published patient cohort that was treated with crizotinib included only one specified patient whose tumor expressed *EML4-ALK variant 2* (2). This patient showed an intermediate response of 57%. Thus, analyses of larger cohorts will be required to afford a sufficiently powered analysis of amount and/or duration of response as a factor of individual fusion variants. Further complicating such an analysis is the fact

that *ALK* fusions are currently diagnosed by FISH. Importantly, such FISH assays only allow detecting the general presence of an *ALK* rearrangement but cannot identify which particular *ALK* fusion variant is present. In light of our findings here, it may be necessary to establish more specific diagnostic tests that can specifically identify the *ALK* fusion present. We hope that future studies will monitor patient outcomes according to specific *ALK* variant status, which would allow us to address this question.

In summary, we found that different *EML4-ALK* variants as well as other *ALK* fusion genes exhibit differential sensitivity to ALK inhibition. In addition, the sensitivity to HSP90 inhibition varied substantially depending on the respective *ALK* fusion and could be further enhanced by combined ALK/HSP90 inhibitor treatment. Such combinations might therefore be promising to test in the clinic. Furthermore, dosing of ALK and HSP90 inhibitors might need to be adapted to specific genetic variants of *EML4-ALK* to enhance tumor control.

Disclosure of Potential Conflicts of Interest

C.M. Lovly is a consultant and an advisory board member of Abbott. W. Pao is a recipient of commercial research grant from AstraZeneca, Enzon, Symphogen, and Xcovery. He is also a consultant and an advisory board member of MolecularMD, AstraZeneca, Bristol-Myers Squibb, Symphony Evolution, Clovis Oncology. R.K. Thomas has received commercial research grant from AstraZeneca, Merck, EOS. He is also a consultant and an advisory board member of Sanofi-Aventis, Merck, Bayer, Lilly, and Roche. Boehringer Ingelheim, Johnson & Johnson, AstraZeneca, Atlas-Biolabs. No potential conflicts of interest were disclosed by the other authors.

Acknowledgments

The authors thank Christian Reinhard, Martin Vabulas, and Ulrich Hartl for helpful discussions.

Grant Support

This work was supported by the German Ministry of Science and Education (BMBF) as part of the NGFNplus program (grant 01GS08100 to R.K. Thomas), by the Max Planck Society (M.I.F.A.NEUR8061 to R.K. Thomas), by the Deutsche Forschungsgemeinschaft (DFG) through SFB832 (TP6 to R.K. Thomas), EU-Framework Programme CURELUNG (HEALTH-F2-2010-258677; to R.K. Thomas), the Behrens-Weise Foundation and by an anonymous foundation to R.K. Thomas. W. Pao acknowledges the VICC Cancer Center Core grant (P30-CA68485) and the Vanderbilt Specialized Program of Research Excellence in Lung Cancer grant (CA90949). C.M. Lovly was additionally supported by an NIH T32 training grant (5T32 CA119910-04), a Uniting Against Lung Cancer grant, and an ASCO YIA.

The costs of publication of this article were defrayed in part by the payment of page charges. This article must therefore be hereby marked *advertisement* in accordance with 18 U.S.C. Section 1734 solely to indicate this fact.

Received December 19, 2011; revised April 25, 2012; accepted May 28, 2012; published OnlineFirst August 21, 2012.

References

1. Soda M, Choi YL, Enomoto M, Takada S, Yamashita Y, Ishikawa S, et al. Identification of the transforming EML4-ALK fusion gene in non-small-cell lung cancer. Nature 2007;448:561–6.
2. Kwak EL, Bang YJ, Camidge DR, Shaw AT, Solomon B, Maki RG, et al. Anaplastic lymphoma kinase inhibition in non-small-cell lung cancer. N Engl J Med 2010;363:1693–703.
3. Takeuchi K, Choi YL, Soda M, Inamura K, Togashi Y, Hatano S, et al. Multiplex reverse transcription-PCR screening for EML4-ALK fusion transcripts. Clin Cancer Res 2008;14:6618–24.
4. Koivunen JP, Mermel C, Zejnullahu K, Murphy C, Lifshits E, Holmes AJ, et al. EML4-ALK fusion gene and efficacy of an ALK kinase inhibitor in lung cancer. Clin Cancer Res 2008;14:4275–83.
5. Soda M, Takada S, Takeuchi K, Choi YL, Enomoto M, Ueno T, et al. A mouse model for EML4-ALK-positive lung cancer. Proc Natl Acad Sci U S A 2008;105:19893–7.
6. FDA news release, August 26. Silver Spring, MD. U.S. Food and Drug Administration 2011.
7. Morris SW, Kirstein MN, Valentine MB, Dittmer KG, Shapiro DN, Saltman DL, et al. Fusion of a kinase gene, ALK, to a nucleolar protein gene, NPM, in non-Hodgkin's lymphoma. Science 1994;263:1281–4.
8. Takeuchi K, Choi YL, Togashi Y, Soda M, Hatano S, Inamura K, et al. KIF5B-ALK, a novel fusion oncokinase identified by an immunohistochemistry-based diagnostic system for ALK-positive lung cancer. Clin Cancer Res 2009;15:3143–9.
9. Choi YL, Soda M, Yamashita Y, Ueno T, Takashima J, Nakajima T, et al. EML4-ALK mutations in lung cancer that confer resistance to ALK inhibitors. N Engl J Med 2010;363:1734–9.
10. Sasaki T, Rodig SJ, Chirieac LR, Janne PA. The biology and treatment of EML4-ALK non-small cell lung cancer. Eur J Cancer 2010;46:1773–80.
11. Pollmann M, Parwaresch R, Adam-Klages S, Kruse ML, Buck F, Heidebrecht HJ. Human EML4, a novel member of the EMAP family, is essential for microtubule formation. Exp Cell Res 2006;312:3241–51.
12. Sharma SV, Bell DW, Settleman J, Haber DA. Epidermal growth factor receptor mutations in lung cancer. Nat Rev Cancer 2007;7:169–81.
13. Kancha RK, von Bubnoff N, Peschel C, Duyster J. Functional analysis of epidermal growth factor receptor (EGFR) mutations and potential implications for EGFR targeted therapy. Clin Cancer Res 2009;15:460–7.
14. Soria JC, Mok TS, Cappuzzo F, Janne PA. EGFR-mutated oncogene-addicted non-small cell lung cancer: current trends and future prospects. Cancer Treat Rev 2012;38:416–30.
15. Yuza Y, Glatt KA, Jiang J, Greulich H, Minami Y, Woo MS, et al. Allele-dependent variation in the relative cellular potency of distinct EGFR inhibitors. Cancer Biol Ther 2007;6:661–7.
16. Greulich H, Chen TH, Feng W, Janne PA, Alvarez JV, Zappaterra M, et al. Oncogenic transformation by inhibitor-sensitive and -resistant EGFR mutants. PLoS Med 2005;2:e313.
17. Sos ML, Koker M, Weir BA, Heynck S, Rabinovsky R, Zander T, et al. PTEN loss contributes to erlotinib resistance in EGFR-mutant lung cancer by activation of Akt and EGFR. Cancer Res 2009;69:3256–61.
18. Sos ML, Rode HB, Heynck S, Peifer M, Fischer F, Kluter S, et al. Chemogenomic profiling provides insights into the limited activity of irreversible EGFR Inhibitors in tumor cells expressing the T790M EGFR resistance mutation. Cancer Res 2010;70:868–74.
19. Heuckmann JM, Holzel M, Sos ML, Heynck S, Balke-Want H, Koker M, et al. ALK mutations conferring differential resistance to structurally diverse ALK inhibitors. Clin Cancer Res 2011;17:7394–401.
20. Lovly CM, Heuckmann JM, de Stanchina E, Chen H, Thomas RK, Liang C, et al. Insights into ALK-driven cancers revealed through development of novel ALK tyrosine kinase inhibitors. Cancer Res 2011;71:4920–31.
21. Takezawa K, Okamoto I, Nishio K, Janne PA, Nakagawa K. Role of ERK-BIM and STAT3-survivin signaling pathways in ALK inhibitor-induced apoptosis in EML4-ALK-positive lung cancer. Clin Cancer Res 2011;17:2140–8.
22. Xu C, Min J. Structure and function of WD40 domain proteins. Protein Cell 2011;2:202–14.
23. Normant E, Paez G, West KA, Lim AR, Slocum KL, Tunkey C, et al. The Hsp90 inhibitor IPI-504 rapidly lowers EML4-ALK levels and induces tumor regression in ALK-driven NSCLC models. Oncogene 2011;30:2581–6.

24. Chen Z, Sasaki T, Tan X, Carretero J, Shimamura T, Li D, et al. Inhibition of ALK, PI3K/MEK, and HSP90 in murine lung adenocarcinoma induced by EML4-ALK fusion oncogene. Cancer Res 2010;70: 9827–36.
25. Katayama R, Khan TM, Benes C, Lifshits E, Ebi H, Rivera VM, et al. Therapeutic strategies to overcome crizotinib resistance in non-small cell lung cancers harboring the fusion oncogene EML4-ALK. Proc Natl Acad Sci U S A 2011;108:7535–40.
26. Peifer M, Weiss J, Sos ML, Koker M, Heynck S, Netzer C, et al. Analysis of compound synergy in high-throughput cellular screens by population-based lifetime modeling. PLoS One 2010;5: e8919.